Design and tests of a three finger hand with 1-DOF articulated fingers

Marco Ceccarelli, Nestor Eduardo Nava Rodriguez*
and Giuseppe Carbone†

*LARM: Laboratory of Robotics and Mechatronics, DiMSAT – University of Cassino, Via Di Biasio 43,
03043 Cassino (Fr) (Italy)*

SUMMARY

This paper presents the design of a new low-cost, easy operation hand having three 1-dof anthropomorphic fingers of a human size. Experimental results on human cylindrical grasping have been used for designing a 1-dof anthropomorphic finger of a human size. The mechanical design of this finger has been mainly focused on a suitable articulated mechanism. This mechanism transmits the power to the phalanxes for a human-like grasping motion and it can be embedded in the body of the finger itself. The design of a three finger hand has been presented as based on the designed finger module. Experimental tests on a built hand prototype have been carried out in order to show the feasibility of the proposed design and validate its operation.

KEYWORDS: Anthropomorphic fingers; Mechanical design; Grasping objects.

I. INTRODUCTION

Several researchers have investigated different types of devices for achieving the grasping and handling of objects. Mechanical grippers having two fingers are widely used in industrial application and, mostly, in industrial robots.[1] However, multi-fingered robotic devices and hands have been also widely investigated, as reported for example in references [2–15]. This type of devices tries to mimic the performances of human hands in order to make high flexibility multi-purpose devices. Significant examples can be identified in the Stanford/JPL hand,[5] the TUAT/Karlsruhe Humanoid Hand,[6] the DLR's Hand II,[7] the BUAA/Bejing University four-fingered hand,[8] Manus Colobi,[9] the TBM hand,[10] the Barrett Hand,[11] and the hands proposed in references [12], [13] and [14] Most of the available multi-fingered prototypes have a high number of degrees of freedom, a complex control and a high cost. The proposed hand is low-cost and easy-operation that means the new prototype has been built with commercial components and it can be controlled easily. Moreover, the new drive-finger mechanism for a 1-DOF anthropomorphic finger can be imbedded in the finger body and it remains in the finger body during its movement. In the recent past, design and research activities have been carried out at LARM, Laboratory of Robotics and Mechatronics, in Cassino in order to design a low-cost, easy operation anthropomorphic finger having 1-dof, as outlined in references [15–21]. A preliminary prototype that has been built at LARM is shown in Fig. 1. The size of this prototype is about 1.5 times bigger then the average human finger.

This paper reports the design and test of a new robotic hand with three anthropomorphic fingers of human size. In the previous papers a different hand of bigger size has been investigated. Experiments with the three fingered hand prototype has been presented in this paper. Special care has been addressed to the design of a suitable transmission system embedded in the body of the finger by using articulated mechanisms. A three finger hand has been also designed and built at LARM by using the designed finger module. Experimental tests have been carried out on human grasping and on the built hand. The comparison of the experimental results can validate the design and operation of the built hand.

II. EXPERIMENTAL TESTS OF HUMAN GRASP

For the design of an anthropomorphic hand a suitable knowledge of the human grasp can be very useful. In particular, dimensions of fingers, grasping forces and contact points between fingers and objects have been investigated in human grasping for design purposes of a new low-cost easy operated hand.

As a first step, several videos of the human hand grasping have been processed. Kinematic models of the fingers have been derived from the analysis of the human grasping, as proposed in Fig. 2. The dimensions of each phalanx of index, medium and thumb have been measured for five persons. The measured values and average values have been obtained, as reported in Table I, referring to the kinematic models of Fig. 2. It is worth noting that it has been decided to measure only the index, medium and thumb since they are the most used in human grasping.

By analyzing several videos of the human cylindrical grasping of a given object it has been observed that there are almost constant ratios between the motions of each phalanx in

* Visiting student at LARM during Academic Year 2002–03 from University of Los Andes in Merida, Venezuela.
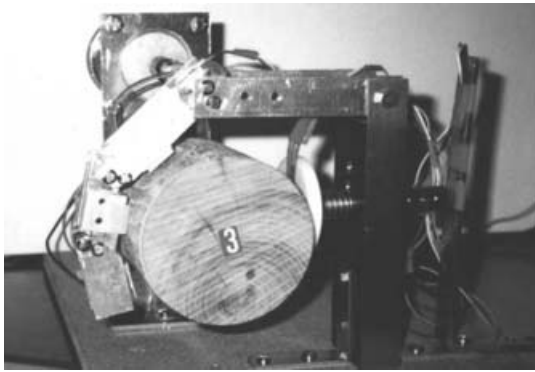† Corrosponding author. E-mail: carbone@unicas.it.

Fig. 1. A preliminary prototype of a 1 dof anthropomorphic finger built at LARM in Cassino, [14, 16].

Table II. Joint angles for phalanx links that are obtained from the image processing of human cylindrical grasping shown in Fig. 3.

Phase	(a)	(b)	(c)	(d)	(e)
θ_1 [deg]	9.7	23.9	46.8	69.9	79.9
θ_2 [deg]	12.5	38.5	68.5	94.7	137.8
θ_3 [deg]	16.9	44.9	74.4	100.2	182.7

the approaching motion to the object, as reported in reference [21]. The motion of the finger is performed usually with a typical motion that can therefore be reproduced with a suitable 1-dof finger mechanism. This aspect motivates the use of only one motor in order to actuate all the phalanxes of a robotic finger since it can give a considerable reduction of costs and complexity of the control. However, it is necessary to properly choose the transmission ratios between phalanxes. The relative positions of the phalanxes have been measured in five different phases of the grasping by carrying out experimental tests and analyzing the images in a CAD environment, as for example Autodesk Inventor.[22]

Figure 3 shows the five phases of the grasping that have been identified. The first phase has been defined as the opening of the hand and moving to the object; the second phase has been determined when the first contact of the finger with the object occurs; the third phase has been determined when there is the second contact between the object and the hand; the fourth phase has been determined the approaching motion of the finger to the object; the fifth phase has been defined as the stable grasping of the object. Marks have been located on the joints of the fingers in order to recognize the displacements during the image processing in the CAD environment. Table II shows the average values of the joint angles as measured during the cylindrical grasping in several experiments similar to the one reported in Fig. 3. Referring to the kinematic model of Fig. 2(a) θ_1, θ_2, and θ_3 are the angles between Lp and Li1, Li1 and Li2, Li2 and Li3, respectively. In particular, Lp is the length of the palm, Li1, Li2 and Li3 are the lengths of the first, second and third phalanx of the index finger.

In order to experimentally measure the grasping forces, six force sensors have been installed on a human hand, as shown in Fig. 4(a). FSR150CP12 sensors,[23] have been used since they are low weight, low cost and easy operation.[16] They have also suitable dimensions as shown in Fig. 4(b) so that they can be glued on a surface of a plastic glove, in order to obtain suitable sensitivity of the sensors as suggested in reference [23].

The overall experimental system has been settled up according to the scheme of Fig. 5. The operation of the sensors has been managed by using an acquisition card AT-MIO-16E-2,[25] and a suitable virtual instrument has been
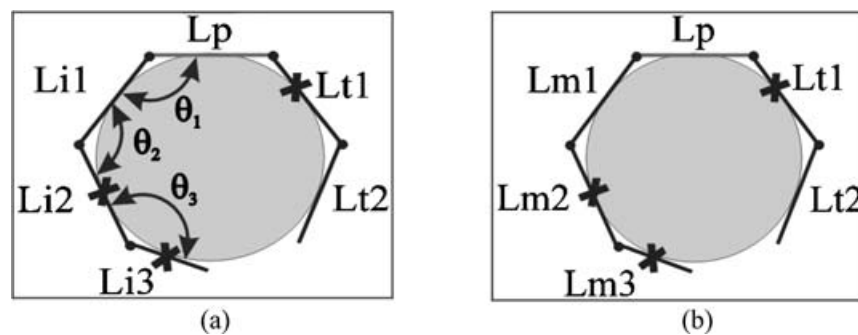

Fig. 2. A kinematic model for human hand fingers: (a) thumb in front of index finger; (b) thumb in front of middle finger (Crosses indicate usual contact points).

Table I. Measured dimensions of human hand fingers referring to the kinematic model of Fig. 2.

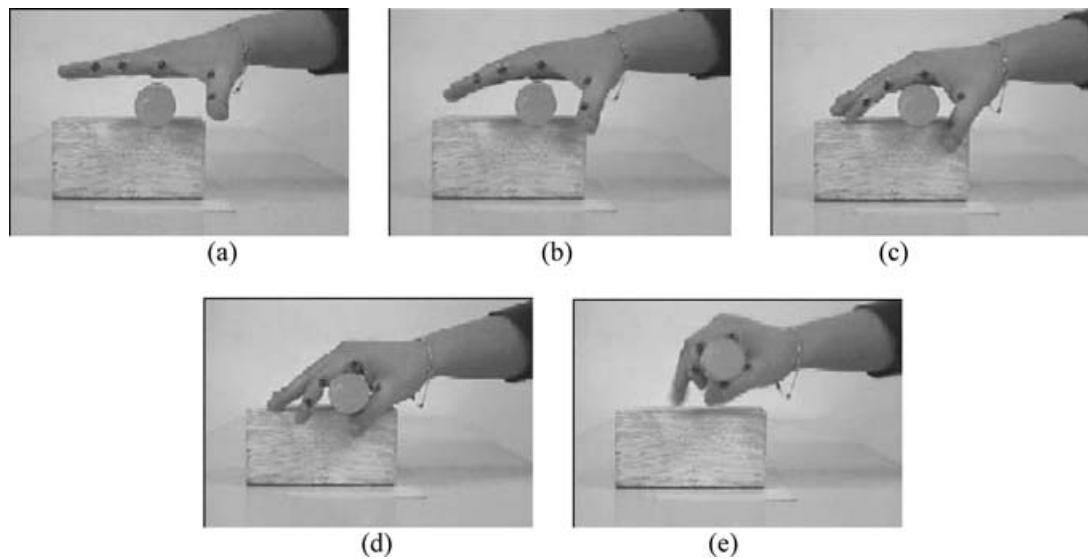| Person	Thumb		Index			Middle		
	Lt1 [mm]	Lt2 [mm]	Li1 [mm]	Li2 [mm]	Li3 [mm]	Lm1[mm]	Lm2 mm]	Lm3[mm]
1	37.7	30.5	25.7	22.5	24.1	28.1	24.9	25.8
2	40.3	34.9	27.4	23.5	22.1	32.5	25.7	28.4
3	39.0	34.7	26.2	19.4	28.8	29.6	23.5	28.8
4	38.3	32.6	27.1	19.2	25.1	29.6	22.2	26.0
5	39.4	33.5	28.3	23.1	25.3	31.7	25.1	27.0
Average	**38.9**	**33.2**	**26.9**	**21.5**	**25.1**	**30.3**	**24.3**	**27.2**

Fig. 3. Phases of a human cylindrical grasping: (a) opening of the hand and moving to the object; (b) first contact of the finger with the object; (c) second contact between the object and the finger; (d) approaching motion of the finger to the object; (e) stable grasping of the object.

developed in a LabView environment.[26] In the experiments the grasping action has been referred to three phases as shown in Fig. 6. In particular, the first phase has been defined when the hand is fully opened and it approaches the object, Fig. 6(a). The second phase concerns with the stable grasp, Fig. 6(b). The third phase is related to the lifting of the grasped object, Fig. 6(c). Figure 7 shows the forces that have been measured in an experimental test by the six force sensors during the grasp of a cubic object of weight 109.6 gr. In particular, Figs. 7(a) and (b) are plots of the forces measured by sensors 1 and 2 that are located on the phalanxes Lt1 and Lt2 of the thumb, respectively. Figures 7(c) and (d) are plots of the forces measured by sensors 3 and 4 that are located on the index phalanxes Li2 and Li3, respectively. Figures 7(e) and (f) are plots of the forces measured by sensors 5 and 6 that are located on the phalanxes Lm2 and Lm3 of the middle finger, respectively. The maximum measured grasping force has been of about 11.0 N, as shown in Fig. 7(b). From the plots of Fig. 7(c), sensor 3 measured

a force near to zero, since the grasp configuration has not given contacts with this sensor. When in contact the grasping forces changes as a function of a static grasp and hand motion. Similar results have been obtained in experiences for grasping object of different shapes and materials. The experiments have been carried out several times by five different persons in order to have a statistical confirmation of values. The results of measured forces with the human hand have been used to validate the operation of the hand prototype, by comparing the measured forces of the human hand with the measured grasp forces of the robotic hand prototype during experimental tests.

III. KINEMATICS DESIGN OF A 1-DOF ANTHROPOMORPHIC FINGER MECHANISM
The results of the experimental tests on the human hand have been used in order to define the kinematic design of a 1-dof anthropomorphic finger. This finger has the same size of the
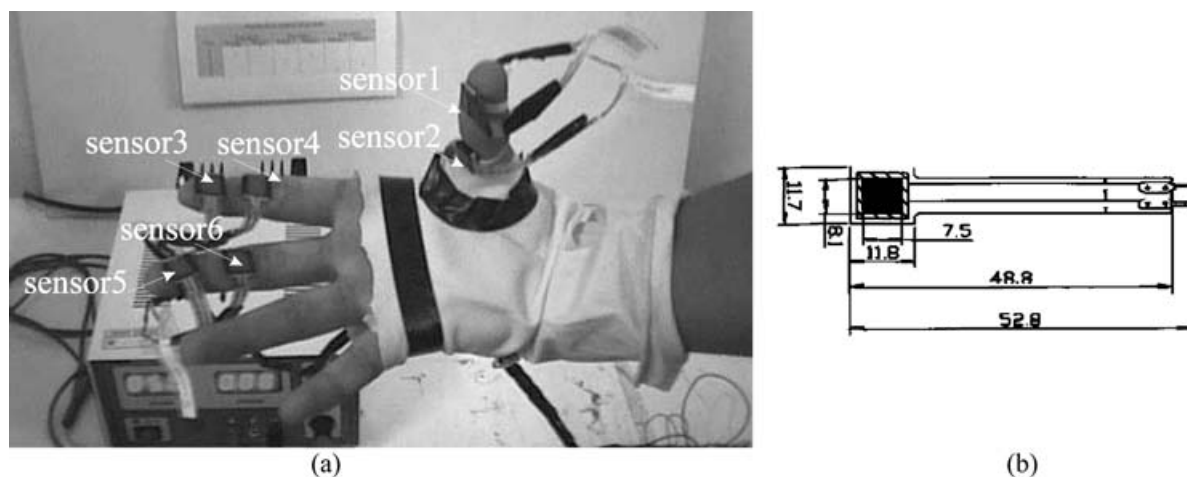

Fig. 4. Sensors installed on a human hand: (a) position of the sensors; (b) FSR150CP12 force sensor with the main dimensions in mm, [15].
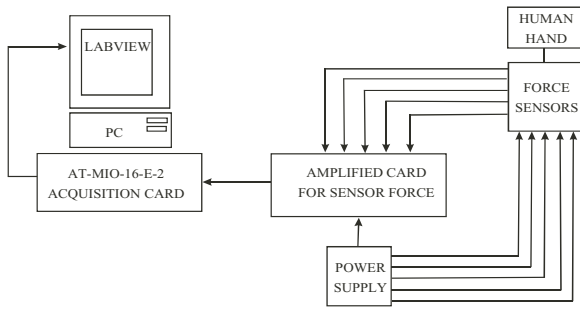
Fig. 5. A scheme for the measuring system for investigating human grasp experimentally.

average human index finger. In particular, data reported in Table I have been used in order to choose the link lengths of the phalanxes that are defined as the distances A_0A_1, A_1D_1 and D_1E_1 in the kinematic scheme of Fig. 8. This kinematic architecture permits to mimic the movement of human fingers with only 1-dof. It has been decided to actuate the first phalanx corresponding to the links $A_0A_1A_2$ by connecting it directly to a motor or through a proper gear train. The other phalanxes are actuated by an articulated mechanism that is connected with the previous phalanx. In fact, referring to Fig. 8 one can note that any movement of the first phalanx will actuate the second phalanx $A_1B_1D_1$ through the link B_0B_1. Similarly, any motion of the second phalanx will actuate the third phalanx $D_1E_1C_1$ through the link A_2C_1. In order to obtain a robust suitable stiff mechanical finger design, it has been devised to use an articulated mechanism for driving

the finger prototype. The drive-finger mechanism is a series of crossed-four bar linkages mechanism. The kinematics architecture of the scheme of Fig. 8 permits to mimic the 3-D.O.F. movement of human fingers by running a 1-D.O.F. mechanism movement. The mechanism is robust and low-cost and it can be embedded in the finger body. Nevertheless, special care has been addressed to the dimensional synthesis of the articulated mechanisms in order to obtain the needed transmission ratios, to avoid link interference, and to achieve suitable mobility. This design has been studied and a solution has been obtained with satisfactory results by looking at the different aspects separately, and by achieving a dimensional synthesis of the mechanism with traditional techniques. Table III reports the main dimensions of the designed kinematic chain referring to the scheme of Fig. 8, as obtained by the dimensional synthesis of the articulated mechanism. The dimensional synthesis has been solved to achieve a human-like motion of the finger.

A kinematic analysis of the mechanism in Fig. 8 can be carried out by writing the closure equations for each four bar linkage that composes the mechanism in the form of vector equation as

$$\mathbf{a} + \mathbf{b} + \mathbf{c} + \mathbf{d} = 0 \tag{1}$$
$$\mathbf{f} + \mathbf{g} + \mathbf{h} + \mathbf{l} = 0 \tag{2}$$

Equations (1) can be written in its scalar form as

$$\begin{aligned} a\cos\theta_1 + c\cos\theta_2 + b\cos\theta_4 + d\cos\theta_0 = 0 \\ a\,\text{sen}\,\theta_1 + c\,\text{sen}\,\theta_2 + b\,\text{sen}\,\theta_4 + d\,\text{sen}\,\theta_0 = 0 \end{aligned} \tag{3}$$
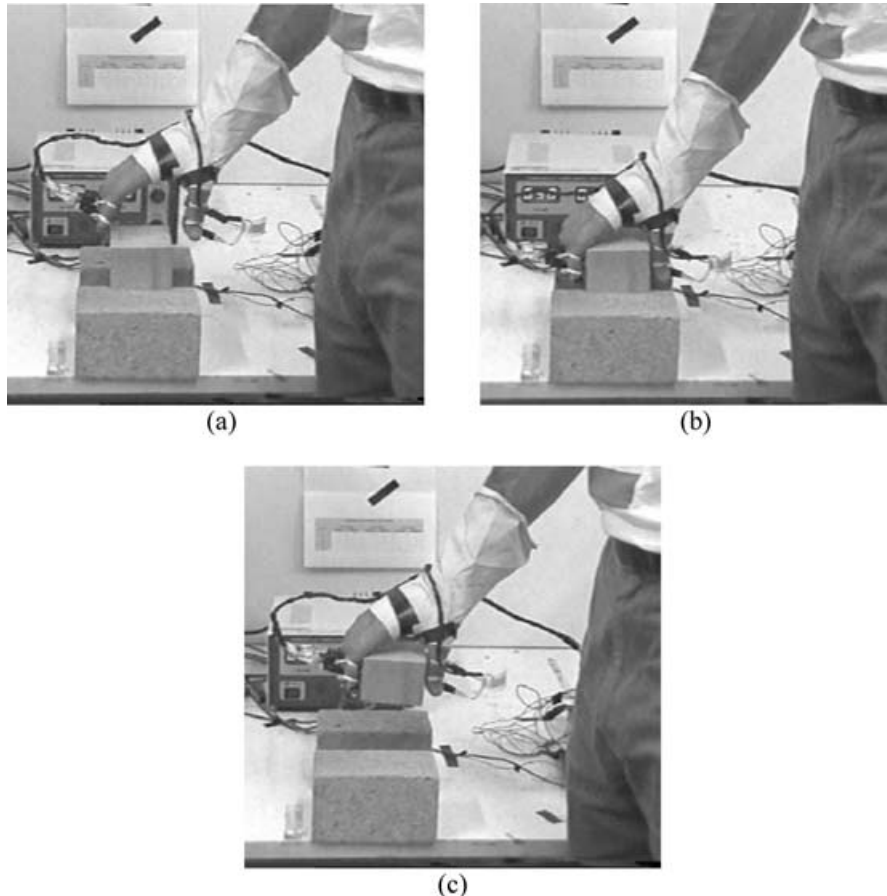

Fig. 6. Grasping phases for force measure in experimental tests: (a) approaching motion; (b) static grasp; (c) lifting the object.
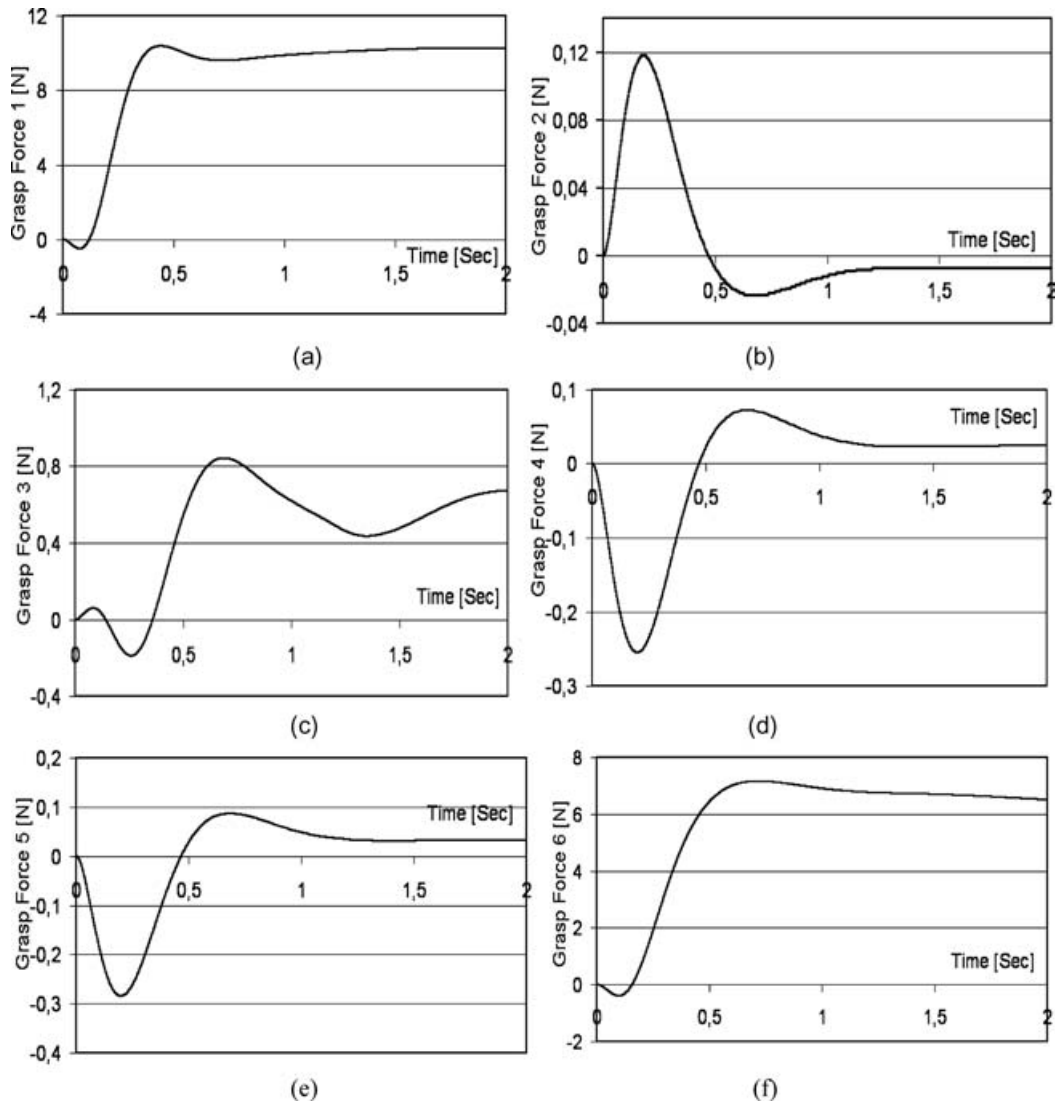
Fig. 7. Plots of the measured forces during the grasping of a cubic object in Fig. 6 by using the sensored grove of Fig.4: (a) by sensor 1; (b) by sensor 2; (c) by sensor 3; (d) by sensor 4; (e) by sensor 5; (f) by sensor 6.
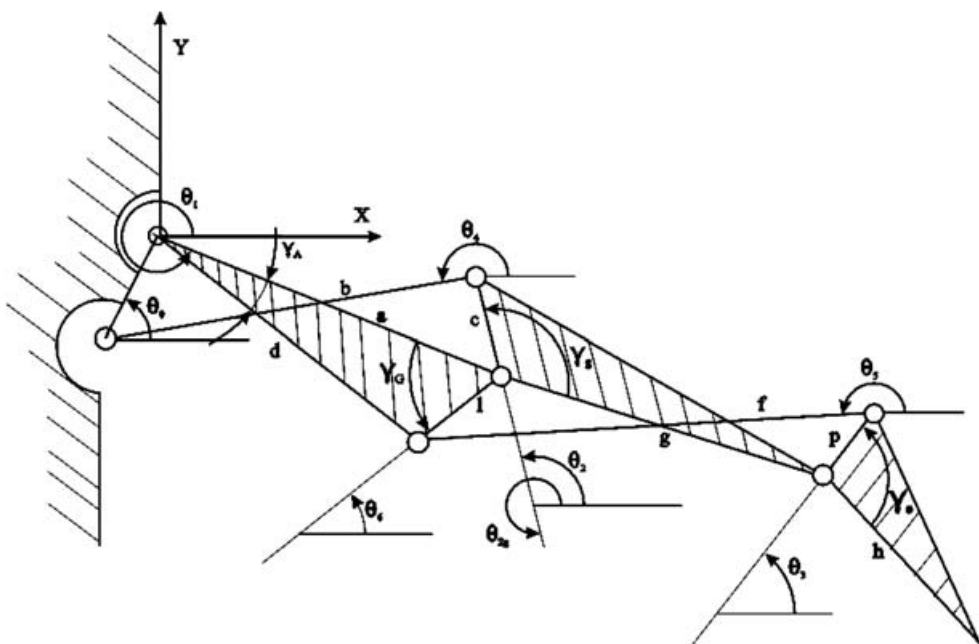

Fig. 8. A design scheme of the articulated mechanism for a 1 dof anthropomorphic finger.

Table III. Dimensions of the new finger prototype with mechanism design of Fig. 8.

Link length [mm]								Angle size [deg]		
A_0A_1	A_1B_1	B_1B_0	A_1A_2	C_1D_1	C_1A_2	A_1D_1	D_1E_1	γ_G	γ_g	γ_e
40.5	5.4	40.9	4.8	5.4	26.0	25.0	23.6	51.0	129.0	127.0

$$g\cos\theta_{2g} + p\cos\theta_3 + f\cos\theta_5 + l\cos\theta_6 = 0$$
$$g\,\text{sen}\theta_{2g} + p\,\text{sen}\theta_3 + f\,\text{sen}\theta_5 + l\,\text{sen}\theta_6 = 0 \quad (4)$$

Taking into account geometrical considerations one can write

$$\theta_{2g} = 2\pi - (\gamma_g - \theta_2); \quad (5)$$

$$\theta_6 = \theta_1 + \gamma_G \quad (6)$$

Equations (3) and (4) can be solved by means of algebraic manipulations when θ_0 is assumed as given constant and θ_1 is considered as the input kinematic variable.

The solutions for equations (3) and (4) can be expressed as

$$\theta_2 = \tan^{-1}\left(\frac{-2C \pm \sqrt{(2C)^2 - 4(A+B)(A-B)}}{2(A+B)}\right) \quad (7)$$

$$\theta_4 = \tan^{-1}\left(\frac{-2E \pm \sqrt{(2E)^2 - 4(D+F)(D-F)}}{2(D+F)}\right)$$

in which

$$\begin{aligned}
A &= (a^2 - b^2 + c^2 + d^2) + 2a\,c\cos(\theta_1 - \theta_0)_{11} \\
B &= 2a\,c\cos\theta_1 + 2c\,d\cos\theta_0 \\
C &= 2a\,c\,\text{sen}\theta_1 + 2c\,d\,\text{sen}\theta_1 \\
D &= (a^2 + b^2 + d^2 - c^2) + 2a\,d\cos(\theta_1 - \theta_0) \\
E &= (2a\,d\cos\theta_1 + 2b\,d\cos\theta_0) \\
F &= (2a\,b\,\text{sen}\theta_1 + 2b\,d\,\text{sen}\theta_0)
\end{aligned} \quad (8)$$

A similar position analysis can be carried out for the second four bar linkage to obtain similar expressions for θ_3 and θ_5.

The functions for θ_2, θ_3, θ_4 and θ_5 like equations (7) have been numerically implemented in order to simulate the operation of the designed mechanism. Figure 9 shows the configurations of the finger when the input angle varies from 0 to 80 deg with a step of 10 deg. Additional results of the kinematic numeral simulation are reported in Fig. 10 as the transmission ratios during the finger motion.

The comparison of the experimental results in Figs. 6 to 7 with the numerical results of simulation in Figs. 9 to 10 shows that the configurations of the phalanxes of the designed mechanism give a good approximation of the cylindrical grasping for an average human finger.

In addition, equations (7) give a velocity analysis of the proposed mechanism in the form

$$\dot{\theta}_2 = -\dot{\theta}_1 \frac{a\,\text{sen}(\theta_4 - \theta_1)}{c\,\text{sen}(\theta_4 - \theta_2)}$$

$$\dot{\theta}_4 = -\dot{\theta}_1 \frac{a\,\text{sen}(\theta_2 - \theta_1)}{b\,\text{sen}(\theta_2 - \theta_4)}$$

$$\dot{\theta}_3 = -\dot{\theta}_{2g} \frac{g\,\text{sen}(\theta_5 - \theta_{2g})}{p\,\text{sen}(\theta_5 - \theta_3)} - \dot{\theta}_6 \frac{l\,\text{sen}(\theta_5 - \theta_6)}{p\,\text{sen}(\theta_5 - \theta_3)}$$

$$\dot{\theta}_5 = -\dot{\theta}_{2g} \frac{g\,\text{sen}(\theta_3 - \theta_{2g})}{f\,\text{sen}(\theta_3 - \theta_5)} - \dot{\theta}_6 \frac{l\,\text{sen}(\theta_3 - \theta_6)}{f\,\text{sen}(\theta_3 - \theta_5)} \quad (9)$$

A further differentiation of equations (9) gives

$$\ddot{\theta}_2 = \frac{-a\cos(\theta_1 - \theta_4)\dot{\theta}_1^2 - b\dot{\theta}_4^2 - c\cos(\theta_2 - \theta_4)\dot{\theta}_2^2 + a\,\text{sen}(\theta_4 - \theta_1)\ddot{\theta}_1}{-c\,\text{sen}(\theta_2 - \theta_4)}$$

$$\ddot{\theta}_3 = \frac{-g\cos(\theta_{2g} - \theta_5)\dot{\theta}_{2g}^2 - f\dot{\theta}_5^2 - p\cos(\theta_3 - \theta_5)\dot{\theta}_3^2}{-p\,\text{sen}(\theta_3 - \theta_5)}$$
$$+ \frac{-l\cos(\theta_6 - \theta_5)\dot{\theta}_6^2 + g\,\text{sen}(\theta_5 - \theta_{2g})\ddot{\theta}_{2g} + l\,\text{sen}(\theta_5 - \theta_6)\ddot{\theta}_6}{-p\,\text{sen}(\theta_5 - \theta_3)}$$

$$\ddot{\theta}_4 = \frac{-c\,\text{sen}\theta_2\ddot{\theta}_2 - a\,\text{sen}\theta_1\ddot{\theta}_1 - \left(a\cos\theta_1\dot{\theta}_1^2 + b\cos\theta_4\dot{\theta}_4^2 + c\cos\theta_2\dot{\theta}_2^2\right)}{b\,\text{sen}\theta_4}$$

$$\ddot{\theta}_5 = \frac{-g\,\text{sen}\theta_{2g}\ddot{\theta}_{2g} - p\,\text{sen}\theta_3\ddot{\theta}_3 - l\,\text{sen}\theta_6\ddot{\theta}_6}{f\,\text{sen}\theta_5}$$
$$+ \frac{-\left(g\cos\theta_{2g}\dot{\theta}_{2g}^2 + p\cos\theta_3\dot{\theta}_3^2 + l\cos\theta_6\dot{\theta}_6^2 + f\cos\theta_5\dot{\theta}_5^2\right)}{f\,\text{sen}\theta_5} \quad (10)$$

Equations (9) and (10) have been implemented in a numerical simulation in order to compute the velocities and accelerations of the phalanxes during the operation of the designed mechanism. In particular, Figs. 11 and 12 show the plots of the velocities and accelerations as function of the input angle for the finger motion of Fig. 9.

A force analysis has been carried out in order to verify that the forces that each phalanx can apply are comparable with the ones that have been measured experimentally on the human fingers. Two cases have been considered, namely, the first case in which it has been assumed that the contact occurs only on one phalanx; a second case in which it has been assumed that all the forces at contact points have same value.

The first force case can be studied through the principle of virtual works and it has been applied referring to the model in Fig. 13. It has been assumed that the resultant of gasping force on each phalanx is applied in the middle of the phalanx itself.

By using this assumption one can write the principle of virtual works as

$$C_m\dot{\theta}_1 = F_1 V_1 + F_2 V_2 + F_3 V_3 \quad (11)$$

The second case of force analysis has been examined as based on the assumption that the grasping force is distributed equally among the three contact points. By using this assumption one can write three expressions

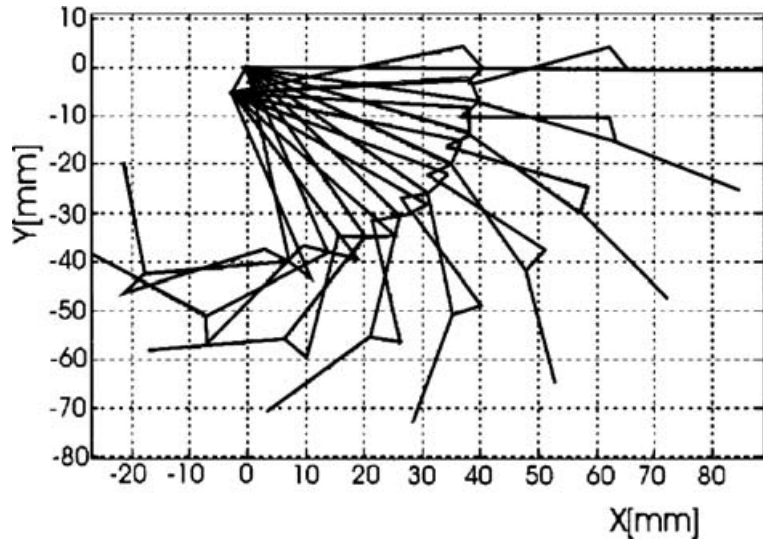$$F_i V_i = \frac{C_m\dot{\theta}_1}{3} \qquad i = 1, 2, 3 \quad (12)$$

Fig. 9. A simulated motion for the designed mechanism mimicking human finger motion.
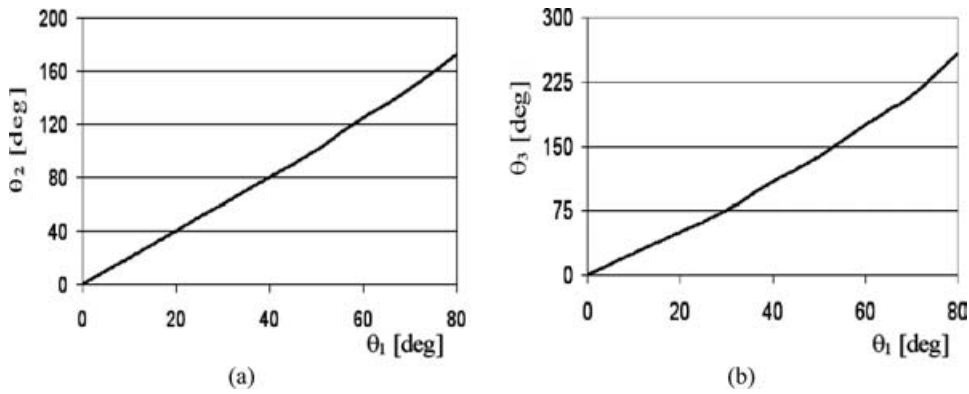

(a)

(b)

Fig. 10. Numerical transmission ratios for the simulated motion of Fig. 9: (a) θ_1 versus θ_2; (b) θ_1 versus θ_3. (the angles are expressed in degrees).
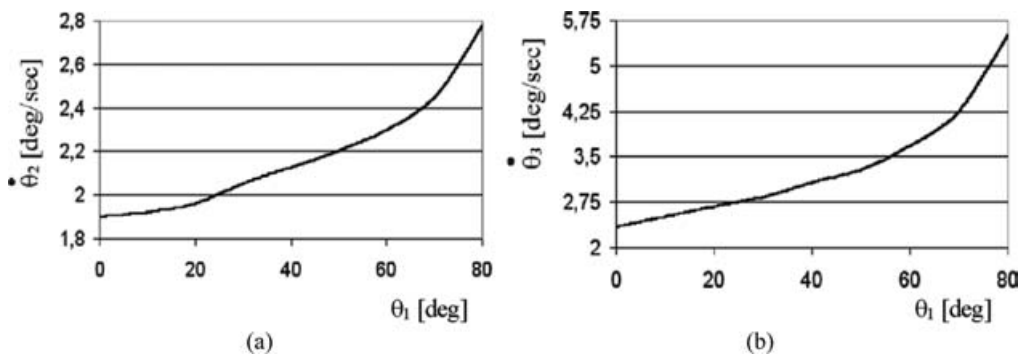

(a)

(b)

Fig. 11. Velocity diagrams for the finger motion of Fig. 9: (a) $\dot{\theta}_1$ versus, (b) θ_2 versus $\dot{\theta}_3$.
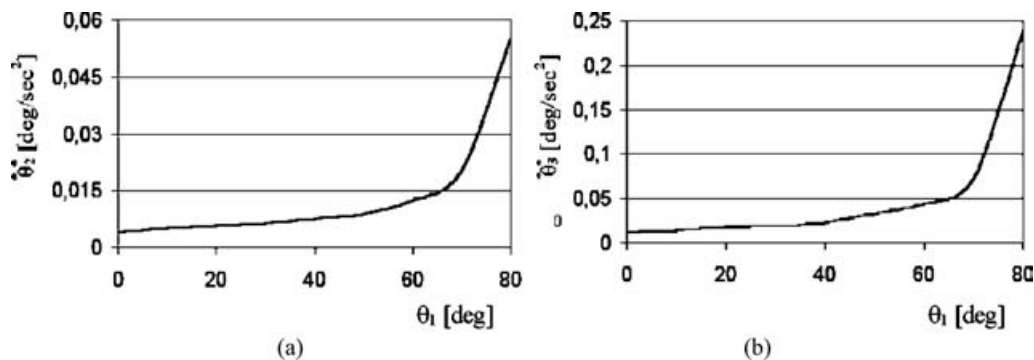

(a)

(b)

Fig. 12. Acceleration diagrams for the finger motion of figure 9: (a) θ_1 versus $\ddot{\theta}_2$, (b) θ_1 versus $\ddot{\theta}_3$.
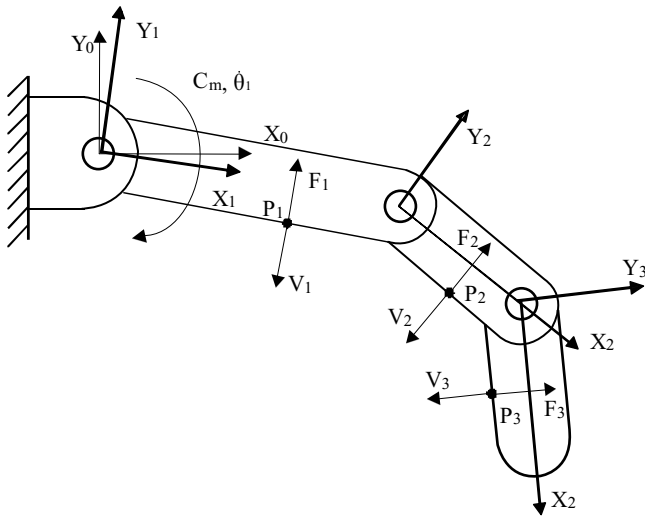
Fig. 13. A model for the forces acting on one finger during cylindrical grasping, assuming one contact for each phalanx.

Figures 14 and 15 show the results of a numerical simulation that has been carried out by implementing Eqs (11) and (12), respectively. It is worth noting that the magnitude of the forces in Fig. 14 is higher then the forces in Fig. 15. In fact, in the case of Fig. 14 the grasp forces are assumed to be applied in the middle of one phalanx. In the case of Fig. 15

the grasp forces are assumed to be applied simultaneously in all the contact points.

IV. A MECHANICAL DESIGN OF A FINGER PROTOTYPE AND A THREE FINGERED HAND

The mechanical design of the new finger prototype has been based on the kinematic model of Fig. 8. A 3D CAD model has been developed in Autodesk Inventor environment,[22] by considering the sizes of the links in the kinematic model. It has been decided to use commercial aluminum alloy for manufacturing the links since it is low-cost and lightweight. It has been also decided to embed the articulated parallelograms that transmit the motion inside the finger body in order to have a compact design.

The developed 3D model has been used in order to check the feasibility of assembling all the components. Figure 16 shows a detail of the assembling of all the components of the fingers. Moreover, the developed 3D model has been used in order to carry out several simulations of the operation of the finger. These simulations have been useful in order to check the feasibility of the proposed dimensions for avoiding any link interference and for properly mimicking the human index finger motion, as reported in Fig. 17. Figure 18 shows a comparison of the designed 3D model with a built prototype.

A three fingers robotic hand has been designed by using the new 1-dof finger module. The results obtained in the
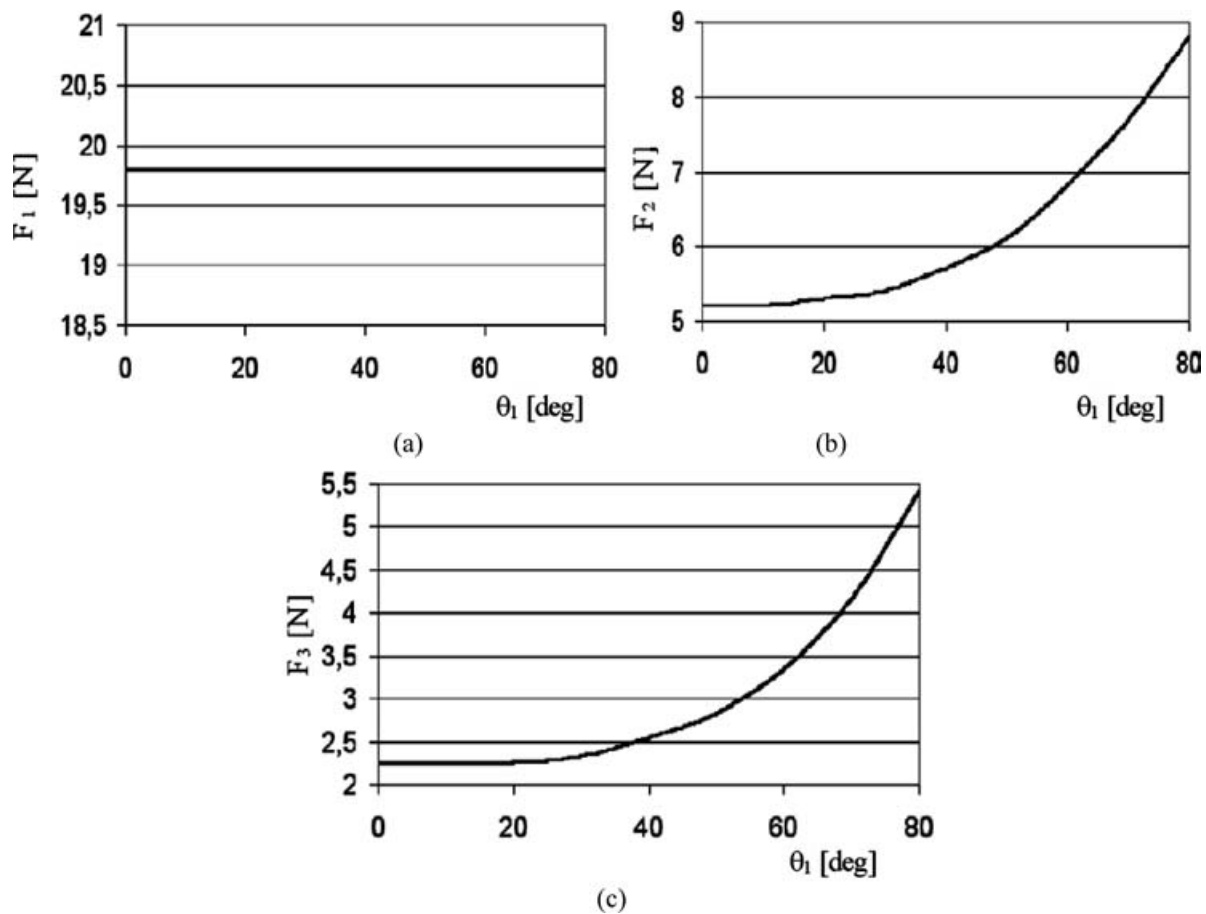

Fig. 14. Results of the first numerical simulation of grasping force: (a) F_1 versus θ_1 (when the only contact point is P_1); (b) F_2 versus θ_1 (when the only contact point is P_2); (c) F_3 versus θ_1 (when the only contact point is P_3).
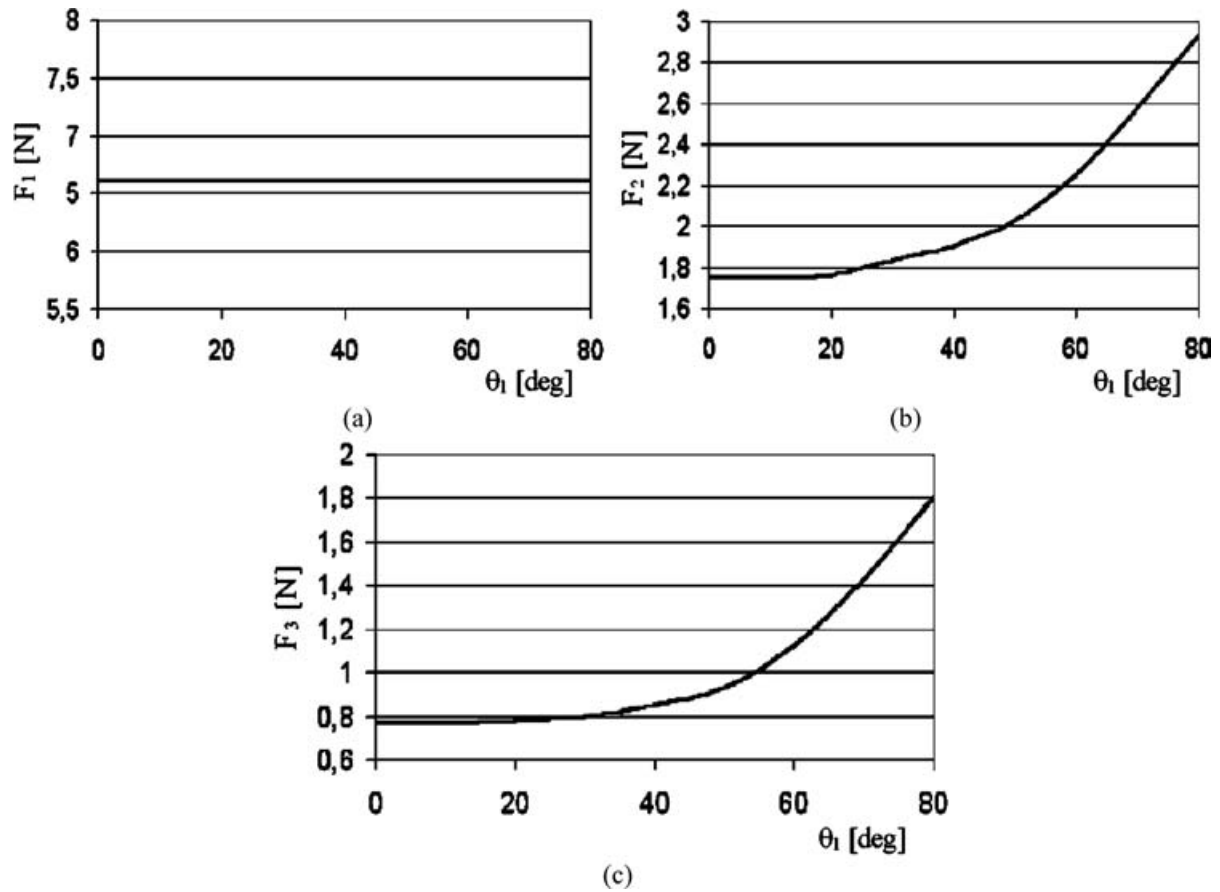
Fig. 15. Results of the second numerical simulation of grasping force (when the grasp forces are applied simultaneously in all the contact points): (a) F_1 versus θ_1; (b) F_2 versus θ_1; (c) F_3 versus θ_1.
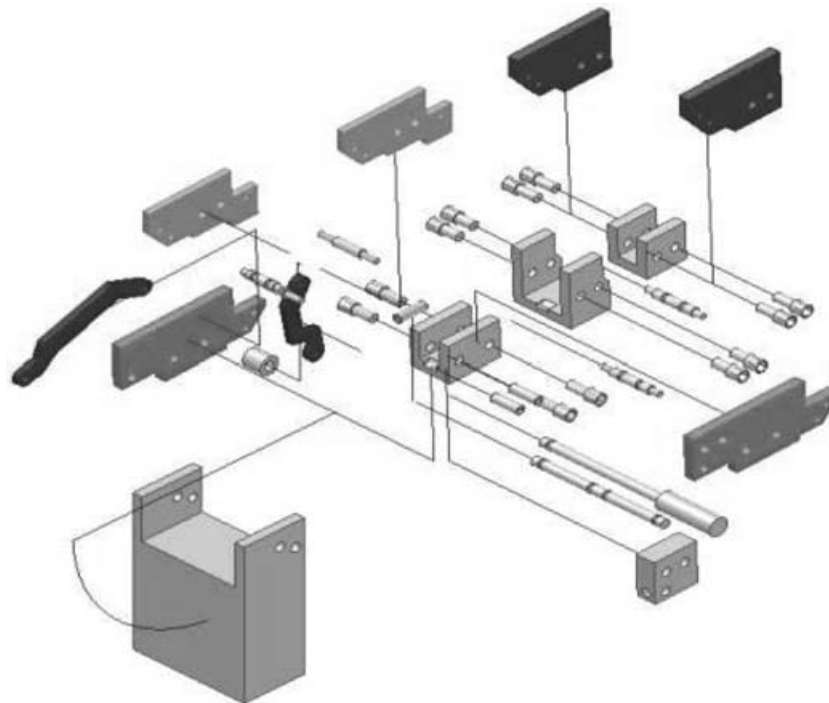

Fig. 16. Parts of the new 1 dof articulated finger of Fig. 8.

tests of grasping, which have been carried out with the human hand at LARM, have been taken into account for the design. Each mechanical component of the hand has been designed by using the Autodesk Inventor, for the analysis of mechanical interference and to simulate the grasping, before the construction of the prototype.
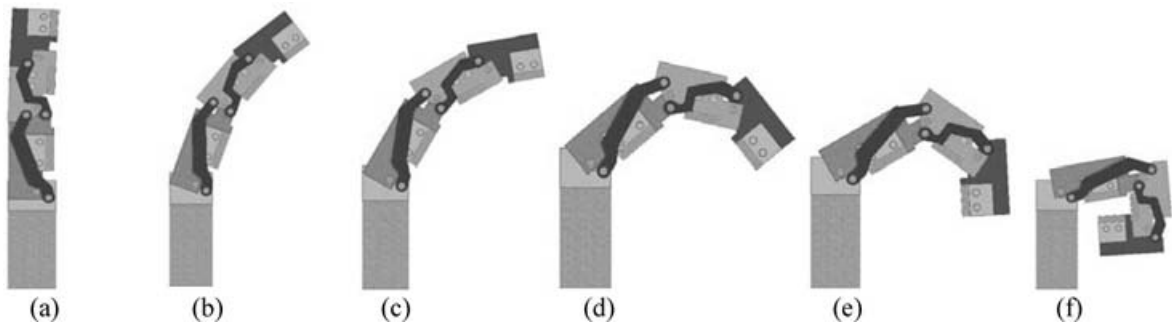
Fig. 17. CAD simulation of the closing movement for the designed 1 dof finger, referring to the configuration in Fig 9: (a) $\theta_1 = 0$ deg; (b) $\theta_1 = 20$ deg; (c) $\theta_1 = 40$ deg; (d) $\theta_1 = 60$ deg; (e) $\theta_1 = 80$ deg.
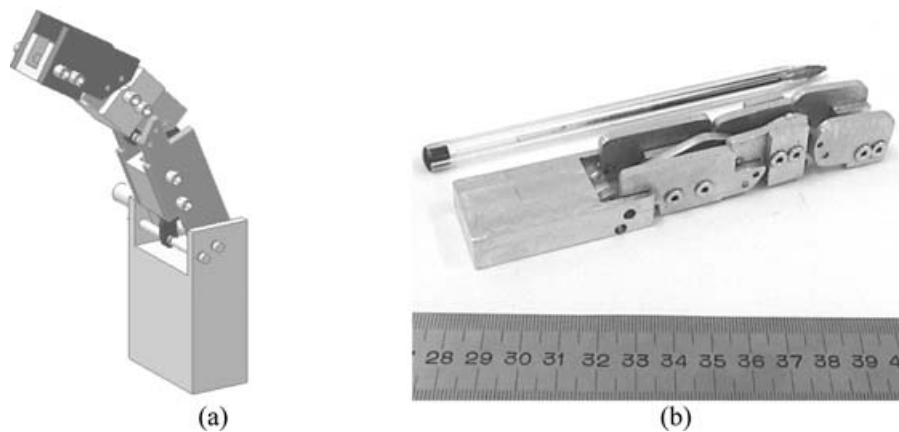

Fig. 18. The new 1dof finger module: (a) a 3D-CAD scheme; (b) a prototype built at LARM in Cassino.
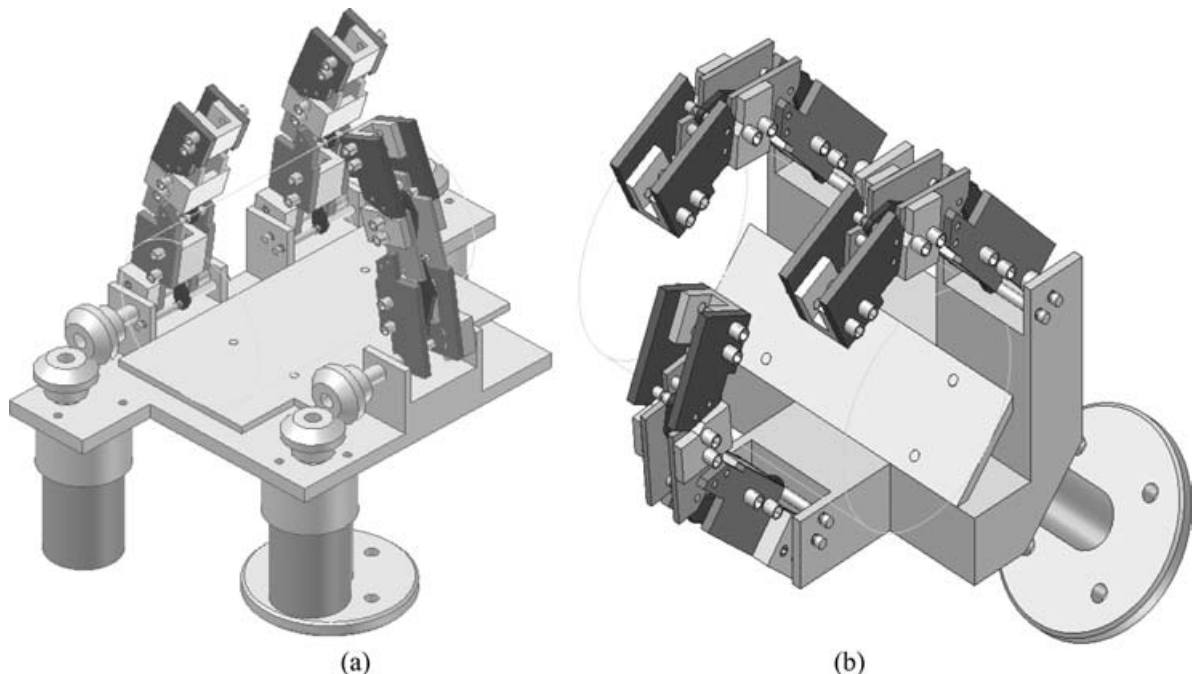

Fig. 19. Proposed designs for a robotic hand with the articulated finger of Figs. 9 and 18: (a) First model, (b) Second model.

Two hand models have been proposed as based on low-cost and compact design constraints as shown in Fig. 19. The principal difference between the first model and the second proposed hand is the design of the palm. In fact, the first hand has a more compact and simple model of palm, as shown in Fig. 19(a). The second hand has a different shape of the palm, as shown in Fig. 19(b). The shape of the palm of the second hand has a different orientation of the fingers and location of actuators respect to the first model hand. These aspects make the second design more anthropomorphic.
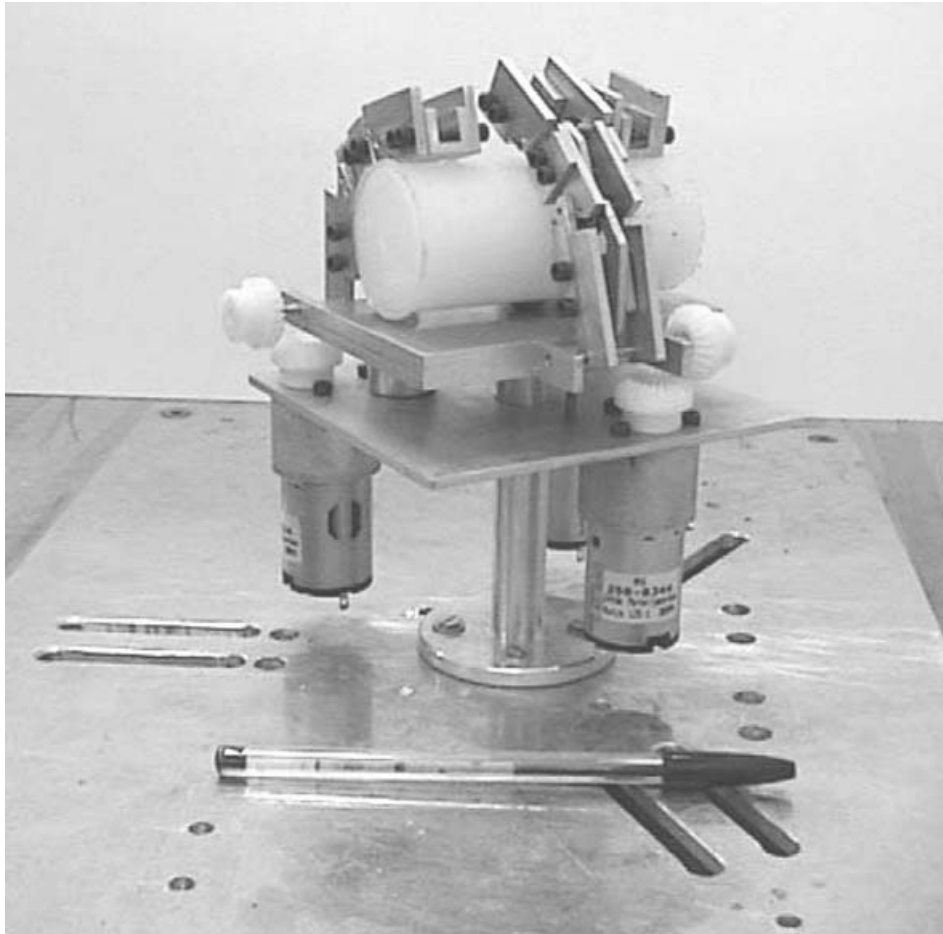
Fig. 20. The new built hand prototype with 3 fingers of human sizes.

Moreover, the actuation of the second proposed hand can be either pneumatic or electric. Figure 20 shows the new hand prototype with 3 fingers of human sizes that has been built at LARM in Cassino.

V. EXPERIMENTS WITH THE THREE FINGERED HAND PROTOTYPE

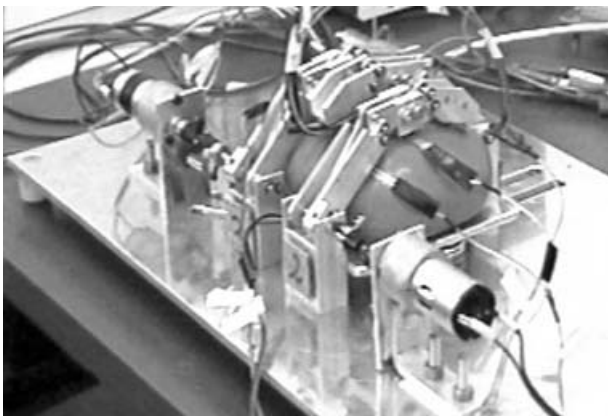Figure 21 shows a test-bed prototype of the proposed anthropomorphic hand that has been assembled with three

Fig. 21. A built test-bed prototype of the proposed hand with three 1 dof anthropomorphic fingers.

1-dof articulated fingers that have been designed and built at LARM in Cassino. The prototype has been constructed by using commercial aluminum bars having U shape side 19 mm, and thickness of 3 mm.

It is worth noting that the contact points between the grasped objects and fingers are not constant depending on the object. In this case we have used a compliant plastic object in order to guarantee the contact between all the phalanxes of the fingers and the grasped objects during experimental tests.

The overall experimental system that is shown in Fig. 4(b) has been settled up according to the scheme of Fig. 5. The operation of the sensors has been managed by using an acquisition card AT-MIO 16E-2,[25] and a suitable virtual instrument that has been developed in LabView environment.[26] Moreover, the operation of the DC motors has been managed by using a PLC LOGO!.[27] It is worth noting that the PLC LOGO! is a low-cost and easy operation PLC that can be programmed by using the commercial software PLC LOGO! Soft.[27]

The PLC LOGO! has been programmed in order to achieve the opening and closing of the hand. In particular, a close loop force control has been implemented by using the signal of the force sensor 1. The motors stop when the grasp force that is measured by sensor 1 is over a threshold value. This threshold value has been chosen as equal to 1,5 N after experimental calibration.
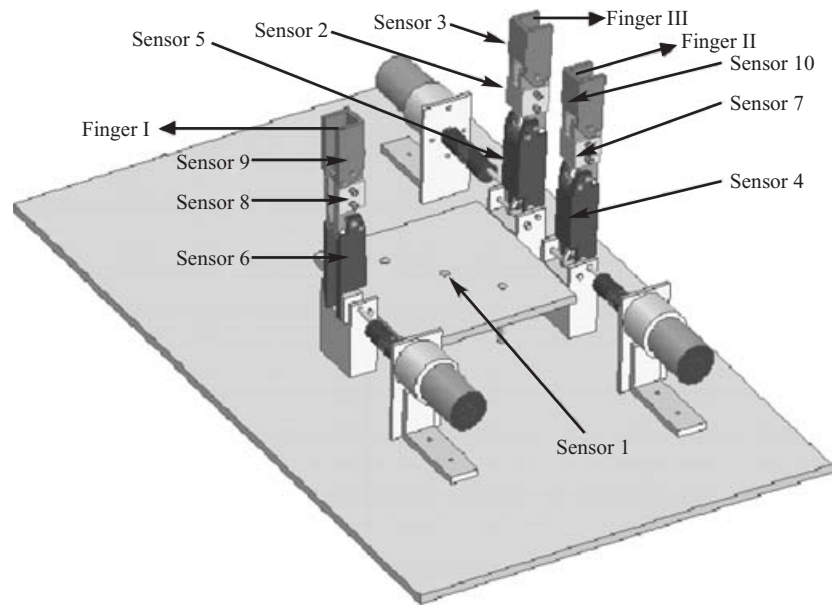
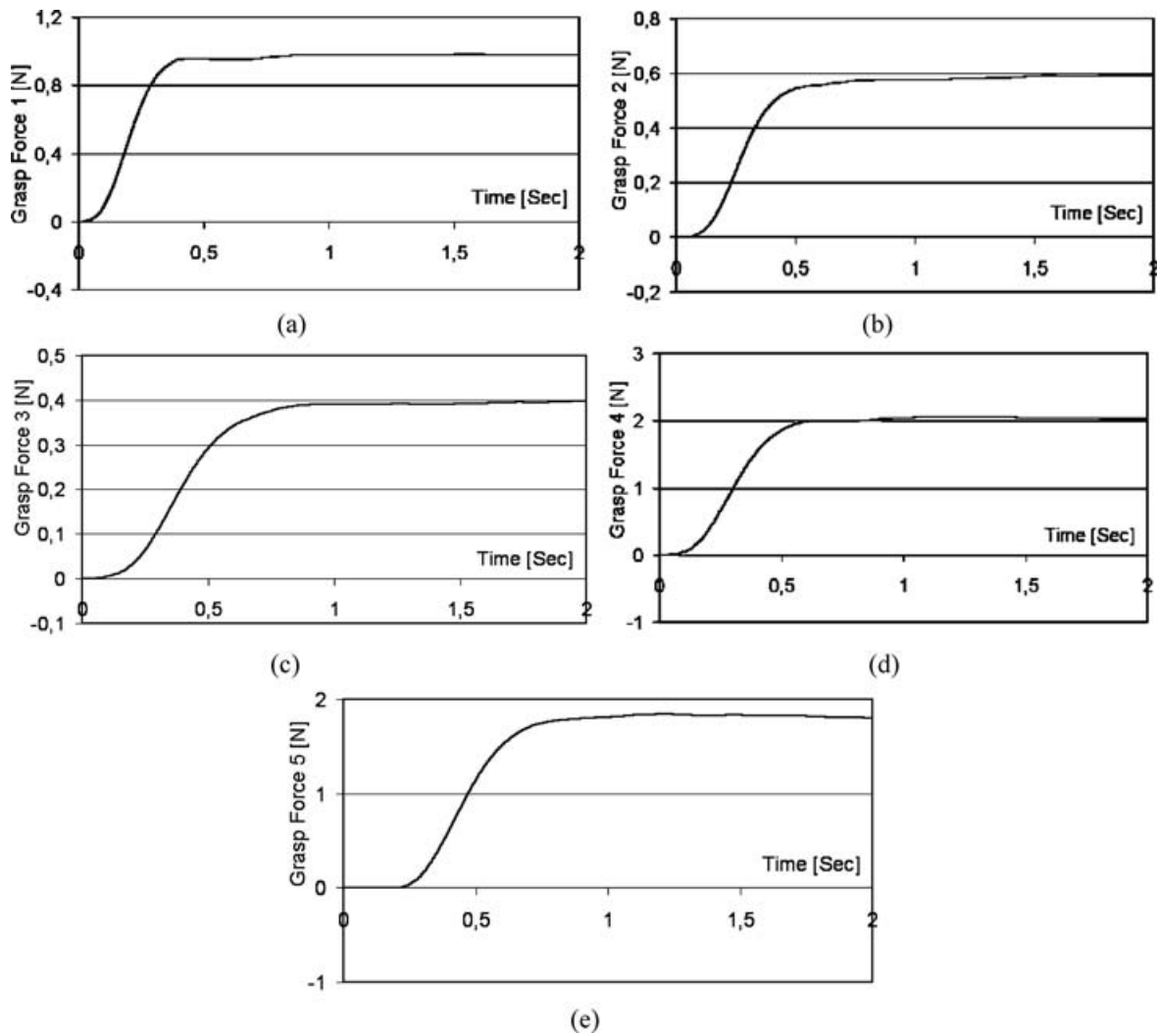Fig. 22. 3D-CAD scheme of the built test-bed prototype with the sensors position.

Fig. 23. Plot of the measured forces during the grasping of an object made by using a compliant plastic object with the hand of Fig. 21: (a) by sensor 1; (b) by sensor 2; (c) by sensor 3; (d) by sensor 4; (e) by sensor 5.
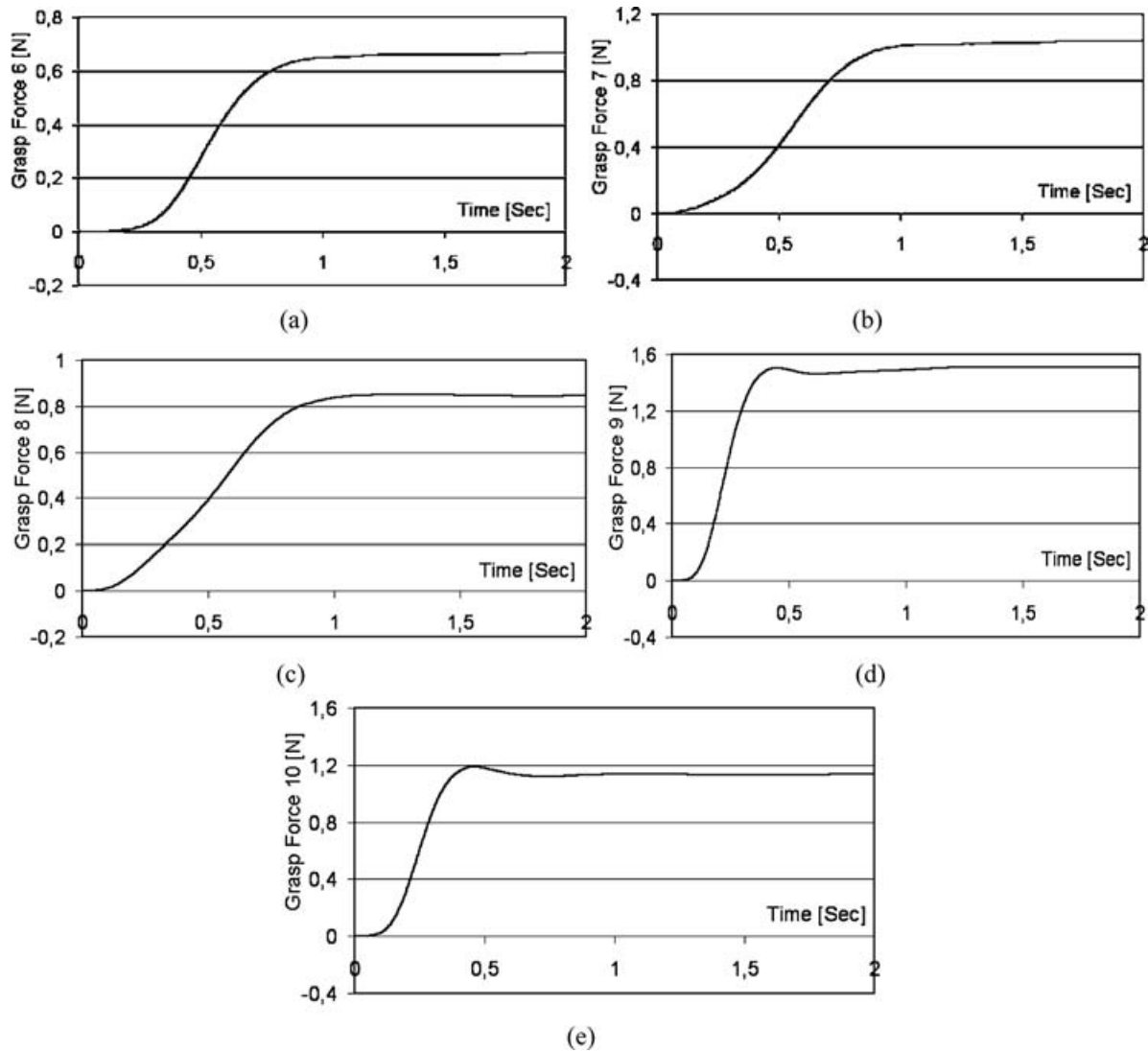
Fig. 24. Plot of the measured forces during the grasping of an object made by using a compliant plastic with the hand of Fig. 21: (a) by sensor 6; (b) by sensor 7; (c) by sensor 8; (d) by sensor 9; (e) by sensor 10.

Figure 23 shows the forces that have been measured by the first five force sensors during the static grasping of an object. In particular, Fig. 23(a) shows the plots of the force measured by sensor 1 on the palm. Figures 23(b), (c) and (e) show the plots of the forces measured by sensors 2, 3 and 5 that are located on the phalanxes 2, 3 and 1 of the finger III, respectively, as shown in Fig. 22. Figure 23(d) shows the plot of the force measured by sensor 4 that is located on the phalanx 1 of the finger II. Figure 24 shows the forces that have been measured by the others five sensors during the static grasping of an object made of compliant plastic. In particular, Figs. 24(b) and (e) are the plots of the forces measured by sensors 7 and 10 that are located on the phalanxes 2 and 3 of the finger II, respectively. Figures 24(a), (c) and (d) are the plots of the forces measured by sensors 6, 8 and 9 that are located on the phalanxes 1, 2 and 3 of the finger I, respectively. The maximum measured grasping force has been about 2 N, as shown in Fig. 23(d).

It is worth noting that the plots of Figs. 23 and 24 show that all sensors have measured a non-zero force, since the grasp has given contacts with all sensors. The experimental tests have been carried out by using a compliant plastic object. This compliant plastic object adapts its geometry to the surface of the phalanxes. Thus, it is possible to have all the sensors in contact with this object. Values of the measured forces equal to zero have been measured by some sensors in experimental tests with rigid objects. In fact, in these tests the grasp has not given contacts with all sensors. This is direct consequence of the rigid structure of the fingers. In fact, the rigid structure of the fingers does not allow the fingers to adapt their geometry to the surface of different objects.

The comparison of the results of the experimental tests on the human grasping and on the above-mentioned three-fingers hand test-bed show satisfactory results. In fact, this comparison validates the operation of the built prototype since the plots of the grasping forces with the human hand and the built prototype have the same shape and comparable magnitudes. The hand prototype shows measured grasping forces that are similar to the human hand for the grasping of different objects, as illustrated in reference [20].

VI. CONCLUSION

In this paper the design of a new hand with 1-dof low-cost easy operation robotic finger has been presented. Particular attention has been devoted to the design of a 1-dof articulated mechanism, which transmits the power from the input shaft to all the phalanxes. Human grasps have been investigated with experimental tests and numerical simulations have been performed in order to design an anthropomorphic finger with human size and human like operation. Experimental tests have been performed in order to validate the operation of the prototype. The experimental results show the practical feasibility of the prototype as a module for a three finger robotic hand, which has been built and tested at LARM in Cassino.

Acknowledgements

References

1. D. T. Pham and W. B. Heginbotham, *Robot Grippers* (IFS Publications Ltd, Bedford, 1986).
2. M. E. Rosheim, "Robot Surrogate: Work in progress", *International Conference on Robotics and Automation*, Minnesota (1996) pp. 399–403.
3. M. R. Cutkosky, "On grasp choice, grasp model, and the design of hands for manufacturing tasks", *IEEE Transactions on Robotics and Automation* **5** (3), 269–279 (1989).
4. T. Iberal, "Human prehension and dexterous robot hands", *Int. J. Robotics Research* **6**(3), 285–299 (1997).
5. J. K. Salisbury, "Design and control of an articulated hand", *International Symposium on Design and Synthesis*, Tokyo (1984) pp. 25–29.
6. N. Fukaya, S. Toyama, T. Asfour and R. Dillmann, "Design of the TUAT/Karlsruhe humanoid hand", *IEEE/RSJ International Conference on Intelligent Robots and Systems*, Takamatsu 3 (2000) **Vol. 3**, pp. 1754–1759.
7. J. Butterfass, M. Grebenstein, H. Liu and G. Hirzinger, "DLR-Hand II: Next generation of a dexterous robot hand", *IEEE International Conference on Robotics and Automation*, Seoul Korea (2001) pp. 109–114.
8. Y. Zhang, Z. Han, H. Zhan, X. Shang, T. Wang and W. Guo, "Design and control of the BUAA four-fingered hand", *IEEE Transactions on Robotics and Automation* (2001) pp. 2517–2522.
9. C. M. Gosselin, S. Mountambault and C. J. Gosselin, "Manus Colobi: Preliminary results on the design of a mechanical hand for industrial applications", *19th ASME Design Automation*, Albuquerque (1993) pp. 585–592.
10. N. Dechev, W. L. Cleghorn and S. Nauman, "Multiple finger, passive adaptive grasp proshetic hand", *Mechanism and Machine Theory* **36**, 1157–1173 (1999).
11. W. T. Townsend, "The barretthand grasper – programmably flexible parts handling and assembly", *Industrial Robot: an international journal* **27** (3), 181–188 (2000).
12. Y. Matusuoka, "The mechanisms in a humanoid robot hand", *Autonomous Robots* **4**, 199–209 (1997).
13. T. Fukuda, K. Mase and F. Arai, "The design and development of a four-fingered robot hand", *IEEE/RSJ International Conference on Intelligent Robots and Systems*, Canada (1998) pp. 482–487.
14. T. Raparelli, G. Mattiazzo, S. Mauro and M. Velardocchia, "Design and develpment of a pneumatic anthropomorphic hand", *Journal of Robotic Systems* **17**(1), 1–15 (2000).
15. S. T. Venkataraman and T. Iberall (Editors), *Dexterous Robot Hands* (Sprinter-Verlag, New York, 1989).
16. G. Figliolini and M. Ceccarelli, "A mechanical design of one D.O.F. anthropomorphic finger based on a human finger motion", *ASME Design Engineering Technical Conferences DETC2000*, Baltimore (2000), CD proceedings, paper MECH-14132.
17. G. Carbone, R. Civitillo and M. Ceccarelli, "Design and test of an articulated mechanism for a 1-dof anthropomorphic finger", *ASME Design Engineering Technical Conferences DETC'02*, Montreal (2002), CD proceedings, paper MECH-34300.
18. M. Ceccarelli, J. M. Jauregui, J. E. Parada, N. E. Nava, C. Lanni and G. Carbone, "Experimental activity for designing a hand with 1 Dof anthropomorphic fingers of human size", *12th International Workshop on Robotics in Alpe-Andria-Danube Region RAAD 2003*, Cassino (2003), CD proceedings, paper 009RAAD03.
19. R. Civitillo, "Design and experimental validation of a 1 dof anthropomorphic finger", *Master Thesis* (LARM, University of Cassino, Italy 2001). (in Italian)
20. J. M. Jauregui, J. E. Parada and N. E. Nava, "Design of an anthropomorphic hand with three 1-dof fingers", *Master Thesis* (Universidad of Los Andes, Mérida, 2002). (Developed at LARM, University of Cassino, Italy). (in Spanish)
21. G. Figliolini and M. Ceccarelli, "Epicyclic gearings and timing belts for an articulated finger", *4th World Congress on Gearing and Power Transmission*, Paris (1999) pp. 2533–2538.
22. Autodesk homepage, "Autodesk inventor 5.3 knowledge modules", http://www.usa.autodesk.com.
23. Konteck Comatel, "Specification sheet for standard lusense sensors of PS[3] family", *Technical Data Sheet* (2001).
24. Interlink Electronics, "FSR integration guide and evaluation parts catalog", *PS – 3 Technical Data Sheet* (2001).
25. National Instruments, "DAQ Acquisition board AT -MIO-16E-2", *General Catalogue* (1995).
26. National Instruments, "LabVIEW 6.0.2", *Users Manual* (1995).
27. Siemens homepage, "Queries related to Logo!", http://www.ad.siemens.de/logo.